Standard PSInSAR approach: Experimental study on the sensitivity of different bounds change on the deformation

Mostafa Ewais[1], Timo Balz[1]

[1]Wuhan University, State Key Laboratory of Information Engineering in Surveying, Mapping and Remote Sensing, Wuhan, China- mustafamagdy724@gmail.com, balz@whu.edu.cn

Keywords: PSInSAR, Temporal Coherence, TerrSAR-X, GPS.

Abstract

An experimental study conducted on standard PSInSAR technique to check the sensitivity of different bounds on the deformation results. This study is motivated by the results obtained from employment of different parameter ranges, with the assumption of the linear behavior of the deformation. despite implementation of slight parameter change shows similarity in most of the PS points. However, significant PS points display slightly different deformation measurements and trends. This change in the PS points motivated an experimental study to evaluate, analyze and assess the results from each different bounds through searching the solution space to find the best fitting to the estimated model, besides assessing of the temporal coherence estimator as quality and fitting indicator. A high-resolution TerraSAR-X (TSX) dataset is used to estimate the deformation using linear model and check the behavior over time. These dataset cover Wuhan city as a case study within two years to avoid non-linearity in the deformation. The main part of this experiment is the descriptive of the statistics across all trials of different bounds. Then, assessing the measurement results of the trials, and the coherence estimator that used as a quality indicator to assess the quality of the PS points in comparison with the standard deviation. The results of the measurements indicate that while the coherence estimator select the PS points based on their stability and fitting to estimated model but does not provide a big difference as function of different bounds through searching the solution space. The results are confirmed with the available global Positioning system (GPS) station in our study area and displays similar trends and patterns over all the trials with slight differences with the different parameters range. The statistical analysis and assessment reveals differences in the velocity results and erroneous during changing the parameters range.

1 Introduction

The standard Permanent Scatterer Interferometry synthetic aperture radar (PSInSAR) technique (Ferretti et al., 2000, 2001) is selecting targets with stable and consistent reflections over time to estimate and retrieve displacement time series. This technique focuses on the coherence of the targets over time series to overcome the limitation in the InSAR that use only two SAR images and avoiding the effects of the atmospheric delays and spatial-temporal decorrelation. Recognizing that certain scatterers exhibit consistent backscatter over time series (Cuenca et al., 2020). According to (Ferretti, 2014) the PSInSAR technique involves two main algorithmic steps. The first step involves unwrapping all differential interferograms. The second step includes estimating and removing atmospheric phase components, followed by identifying the PS points that provide useful information related to deformation. This technique is estimating the deformation velocity mean over a specific time series, arising to accurate estimates of the deformation (Adam et al., 2009). In addition, several studies implemented PSInSAR to monitor and measuring the displacement adopting different deformation models, e.g., linear (Ferretti et al., 2001; Wright et al., 2001), seasonal, quadratic, non-linear deformation (Afzal et al., 2024; Jiang et al., 2021; F. Van Leijen, 2016; F. J. Van Leijen & Hanssen, 2007). Using these models with previous knowledge leads to accurate ambiguities resolving of the phase measurements through assuming a certain model for the movement of the land or targets. The assumption of the deformation model is considering a constraint in the estimation of the parameters to capture the extent of deformation behavior (Verburg, 2017). Standard PSInSAR methodology using the coherence that is the average closeness of the PS phase to a given model (Sousa et al., 2011). This should be consistent within the same deformation model giving similar results, however using the same deformation model with different or change the range of the estimated parameters slightly show some differences in the obtained PS (Permanent scatterers) concerning the velocity value and patterns as shown in Figure 1. Therefore, the aim of this experimental study that is motivated by these differences in results is assessing the quality of the model with different bounds through searching the solution space.

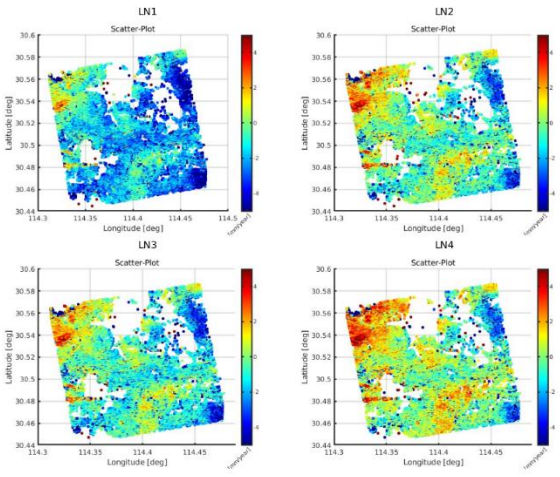

Figure 1. Applying different bounds on TerraSAR-X data using linear model. The velocity rate is color-coded.

2 Materials and Methods

The PS-InSAR technique is employed alongside the SARPROZ software (Perissin et al., 2012; Roccheggiani et al., 2019) to process the datasets using the standard processing as shown in the flowchart in Figure 2.

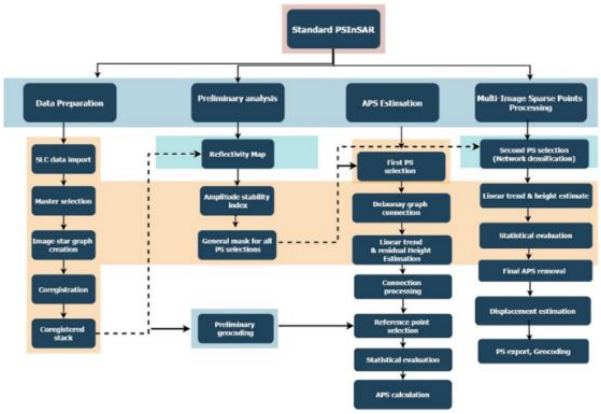

Figure 2. Simplified processing chain of the standard PSInSAR technique in SARPROZ.

2.1 SAR Datasets

In this investigation, the processing was based on a set of high-resolution images of TerraSAR-X images from ascending satellite track covering the period February 3, 2016, to December 16, 2017. a set 29 ascending images, acquired with HH (horizontal transmit and horizontal receive) polarization and an incidence angle of approximately 35.3° at the scene center over Wuhan, the key parameters of the TerraSAR-X data stack employed for the analysis are detailed in Table 1.

Data	TerraSAR-X(TSX)
Temporal coverage	[2016-2017]
Orbit direction	Ascending
Incidence angle	35.3°
Polarization	HH
Number of Images	29

Table 1. characteristics of the TerrSAR-X (TSX) dataset used in this experiment.

2.2 Experimental study

The experimental study is implemented on Wuhan city, largest city located in central China. Wuhan land subsidence was induced by urban development that affecting the infrastructure (Hu et al., 2022). To explore and estimate the linear trend in Wuhan, we used TerraSAR-X datasets with coverage as shown in Figure 3. Deformation and residual height estimations are then conducted within the provided search space. In this study, we estimate the linear deformation using different parameters ranging from +/-40 mm/year to 100 mm/year and for residual height estimation between +/-100 m to +/-250 m. At the end, to remove the falsely detected PS or select the best PS points that fit the model, the ensemble coherence estimator is used that based on deformation time series. The ensemble coherence estimator is a metric to describe the deviation between the deformation time series and the deformation model estimated. For the validation and comparison of the PSInSAR results, GPS is used to compare the displacement results in the Vertical direction. Only one GPS station is available and used in the study area to compare the results. The vertical displacement observations of the GPS are downloaded, within the time series of 2014, from the Nevada Geodetic Laboratory GPS Networks Map website (http://geodesy.unr.edu/).

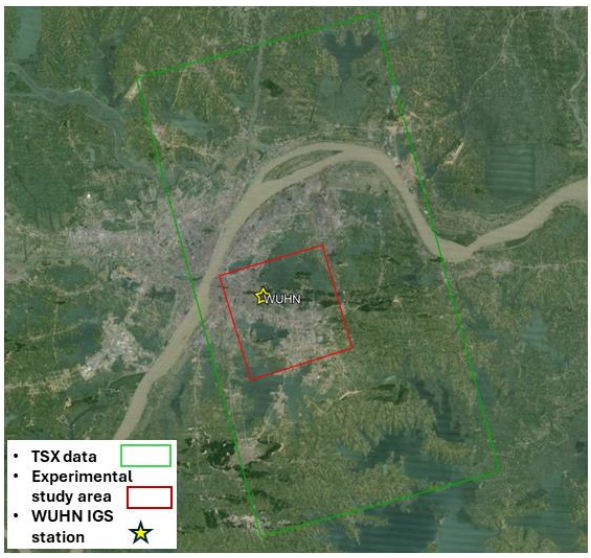

Figure 3. Experimental study area with the coverage of the TerraSAR-X (TSX) data.

3 Results

Configuration to estimate the parameters involves input of different ranges for the residual height and velocity to be estimated based on steady-state model. Different trials have been conducted with the different bounds denoted as LN1 to LN4 for the different ranges as shown in Table 2.

	Trials	Residual height [m]	Velocity [mm/y]	No. pnts [-]	Mean [mm/y]	Med [mm/y]	Std [mm/y]	Skew [-]	Min [mm/y]	Max [mm/y]	Q1 [mm/y]	Q3 [mm/y]
0	LN1	+/-100	+/-40	136294	-1.5784	-1.67	2.7989	6.0928	-52.21	64.46	-2.57	-0.75
1	LN2	+/-150	+/-60	147146	0.0818	-0.01	2.8163	5.2392	-58.12	60.00	-0.92	0.93
2	LN3	+/-200	+/-80	140240	-0.3860	-0.42	2.7758	2.3073	-80.00	80.00	-1.32	0.52
3	LN4	+/-250	+/-100	141535	0.5858	0.58	3.7212	-3.8802	-100.00	99.39	-0.35	1.56

Table 2. statistical analysis of TSX data

3.1 Number of Permanent Scatterer (PS) Points

Permanent scatterers (PS) are coherent targets or point like scatterers that have strong and consistent backscattering. Applying different ranges of the estimated parameters i.e., residual height and velocity, to search the solution space on the same SAR datasets and on the same study area give different numbers of PS points. as shown in Table 2 with changing the bounds through searching the solution space. The number of PS points show variation throughout the four trials, with maximum PS points in LN2 and minimum at LN1.

3.2 Minimum & Maximum velocity

Through increasing the range of the velocity rate, noticing an increase in minimum and maximum values, to search for points fit the predicted model as shown in Table 2. increasing the range is followed by increasing in the rate of velocity as shown in Table 2 and the minimum and maximum values can be inferred from the boxplot Figure 4, for LN4 that show a large minimum and maximum values, -100mm/y and 99.39mm/y, respectively. For the quartile values (Q1&Q3) of LN1 appears with negative sign with 25% of the velocity values below -2.57 mm/yr. and 75% below -0.75 mm/yr., indicating that most of the PS points have negative velocity values. This is also reflected in the scatter plot of the velocity rate of LN1 as shown in Figure 1. conversely to

LN1, all trials have both negative value for Q1 and positive for Q3. For LN2 the Q1 and Q3 are like each other with opposite values. For Q1 LN1 has the highest rate compared to LN4, and for Q3 LN4 has the highest positive rate compared to other positive values among trials. Changing the ranges appear with higher change in the deformation along the study area from the most subsidence as in case of LN1 to more inflation as in case of LN4.

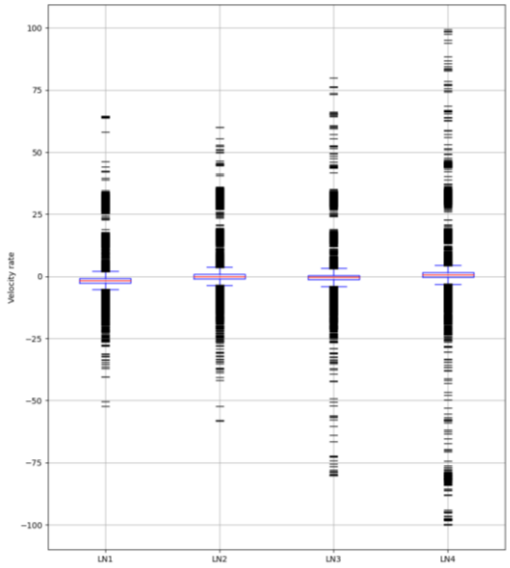

Figure 4. BOXPLOT portraying the distribution of the LOS deformation (mm/yr.)

3.3 Mean and Median velocity

Both statistical terms are measures of the central tendency, hence the mean value is the average value, and the median is the middle value in the data. These two statistical parameters are an indicative of the distribution of the data and display the symmetry or asymmetry of the distribution. The mean and median velocity values per distribution are summarized in Table 2. it noticed that the mean values are negative (LN1&LN3) and positive values (LN2&LN4), indicating a variation of the most of the PS points from subsidence to inflation. For instance, as in LN1 the mean velocity is -1.57 mm/yr., meaning that the velocity values over all 136294 points indicates subsidence. While indicate the opposite for LN2 with rate about 0.08 mm/yr. the lowest mean value is displayed in LN2 and highest value in LN1.meanwhile, the median values are negative in all trials except for LN4, and LN2 is smallest value closer to zero value indicating symmetry in the distribution of the data which also supported by the Q1 and Q3 values and closer of the mean value to the median value compared to other trials.

3.4 Skewness

Skewness is a measure of the asymmetry of the probability distribution of a about its mean. In simpler terms, it indicates whether the data is skewed to the left (negative skewness) or to the right (positive skewness) relative to the mean. It noticed that all the trials have positive skewness except for LN4, indicate that the distribution of the velocity values skewed sequentially in decreasing order to positive values as in LN1, LN2, LN3 trials, portraying more symmetrical in the distribution with increasing the ranges with exception of LN4 that shows negative skewness values concentrated on the lower end of the velocity range.

3.5 Standard Deviation

The standard deviation is a measure of the dispersion or variability of a set of values around their mean and it is quantifying the amount of variation or dispersion present in a dataset (Bland and Altman, 1996). The dispersion can be interpreted and explained as its distance to their mean deformation. Through analysis of the standard deviation values in Trials LN2 and LN4 (highest value) have relatively higher variability values, while Trials LN1and LN3 (lowest value) have lower deviation values. This high value of standard deviation indicates that the velocity values are more widely spread out of the mean value.

3.6 Internal assessing checks

3.6.1 Residual Height

The height Estimation of the PSs are relied on the DEM error at the reference PS. the DEM error is affected by the used reference DEM precision. The DEM portrays the layer where the PS reflection point is located, whether it is a surface model (DSM) incorporating objects or a terrain model (DTM) excluding them. Perfect DEM availability couldn’t be assumed during processing, Consequently, residual DEM heights will consistently impact the double-difference phase observations. Therefore, it is important to estimate the DEM error to resolve the deformation signal. The residuals represent the errors performed by the model for the estimation throughout times series comparatively to the desired ones. The bounds of residual heights are set to ± [100, 150, 200, 250] m. the value of standard deviation of the residual display or measure the spread or dispersion of the residual heights. Higher values indicate greater variability in the residuals and lower values indicate more consistent predictions. In addition, the skew value describes the asymmetry of the residual height distribution. A positive skew value indicates that the distribution has a longer tail towards positive values, while a negative skew suggests a longer tail towards negative values. As shown in Table 3, The standard deviations of all trials have similar values, with higher residual values at LN1 and LN4 (highest value) compared to LN2 (lowest value) and LN3. but the relatively high value indicates uncertainty in the height estimates. In addition, all trials depict positive skewness, especially at LN4, suggests that longer tails toward positive values and indicates a tendency of underestimation of the residual heights.

	trial	Mean of Residual Height[m]	std of Residual Height[m]	Skew of Residual Height[-]
0	LN1	-4.025600	12.000100	1.468500
1	LN2	-0.830900	11.539900	1.205000
2	LN3	-3.034100	11.833700	1.157000
3	LN4	13.563100	12.512200	2.217600

Table 3. mean, standard deviation and skewness of residual height.

3.6.2 Quality Indicators

The quality of the estimated time series deformation and the bounds search the solution space to estimate the unknown parameters can be expressed by temporal coherence and standard deviation of displacements based on steady-state model.

3.6.2.1 Temporal Coherence

The coherence estimator is identified for PS relative to the reference PS. Hence, this reference point is selected based on the assumption that is minimal noise. The value of coherence is an indicator of the scattering noise level of the PS included, atmospheric artifacts and unmodeled deformation. Besides

Temporal coherence is a metric describing the deviation between the deformation model estimated and the deformation time series and identification of the suitable PS points, temporal coherence was employed as quality indicator to assessing the quality of the final PS obtained, which is the goal of this study. As defined in equation (1), the temporal coherence ranges between 0 and 1. The former indicates complete noise, while the latter indicates perfect correlation between the estimated deformation model and the observed deformation. The value of coherence reflects the scattering noise, unmodelled part of the deformation and atmospheric signal delay.

$$|\gamma| = \frac{1}{N-1} 1 \sum_{k=1}^{N-1} e^{(j(\vec{\Phi}_{obs}^{OS} - \vec{\Phi}_{model(b)}^{OS}))} \qquad (1)$$

As displayed in Tables 4 The mean temporal coherence display good mean coherence values around 0.90. The mean coherence value is relatively low at LN2 (0.9). The median of temporal coherence is the same for all trials, except for LN4 make the distribution of values across all trials is similar. The standard deviation values are relatively low in all trials of all datasets, indicates clustering of the temporal coherence around the mean value for each trial of all datasets. The skewness values in all trials of datasets are negatively skewed, indicating the temporal coherence skewed and most of the PS points have high temporal coherence, with longer tails toward lower coherence values. The value of the mean and median are slightly closer to each other, in which the median not affected by the outliers or extremes. The negative skewness indicates that most of the PS points clustered around the higher temporal coherence proves that these points are stable and fitting the model. The value of the skewness is lower in LN2.

	trial	Mean	Median	Standard Deviation	Skew of Temporal Coherence
0	LN1	0.905300	0.920000	0.064000	-1.0656
1	LN2	0.901900	0.920000	0.071200	-1.0299
2	LN3	0.906000	0.920000	0.064900	-1.0625
3	LN4	0.906200	0.930000	0.069400	-1.0861

Table 4. statistical analysis of temporal coherence applied on TSX data.

3.6.2.2 Standard deviation of the deformation

The deviation of the difference between the observed and the predicted deformation model is defined as residual standard deviation. The quantity of the resulted values will be in millimeters rather than a factor such as ensemble coherence estimator. As shown in Tables 5, the mean values are relatively similar throughout all trials and the median values are closer to the mean values. While the standard deviation values are small reflecting low variability in the measurements. In addition, all trials have positive skewness with LN2 and LN4 (highest), LN1 and LN3 lowest skewness. while the values of standard deviation of the residuals in all trials more similar but with slightly differences reflecting the deviation of slightly PS points. As shown in Figure 5, depicting the histograms of the temporal coherence and standard deviation of the PS points for all trials. Despite of the similarity of the shape of the distribution of the PS points but slight bit differences in some PS points with variation in the standard deviations of the trials. Therefore, for more assessing, the variation coefficient is employed Table 6, which is a measure of the variability as a percentage or proportion of the total and it’s calculated as the ratio of the standard deviation to the mean [see equation 2]. It has an advantage in measuring the variability of data sets with different units, even with dimensionless quantity as temporal coherence (Martone et al., 2015). The formula of the Coefficient of variation (CV) is:

$$\mathrm{CV} = \frac{\text{standard deviation}}{\text{mean}} \text{ x } 100 \qquad (2)$$

As noted in Table 4 that the CV is higher for temporal coherence at LN2 and lower for at LN1&3. While for the standard deviation value is lower at LN2 and higher at LN1 &3.

	Trials	Mean [mm/y]	Min [mm/y]	Max [mm/y]	Median [mm/y]	SD [mm/y]	Skew [-]
0	LN1	0.7628	0.68	1.54	0.74	0.0637	1.6374
1	LN2	0.7360	0.68	1.59	0.72	0.0421	2.2949
2	LN3	0.7577	0.68	1.81	0.74	0.0620	1.7792
3	LN4	0.7378	0.68	1.68	0.72	0.0442	2.3075

Table 5. statistical analysis of the standard deviation of the deformation.

	Coefficient of variation (CV)	
Trials	Temporal coherence	Standard deviation of deformation
LN1	7.11	8.28
LN2	7.88	5.75
LN3	7.11	8.26
LN4	7.66	6.02

Table 6. coefficient of variation of the temporal coherence and deformation standard deviation.

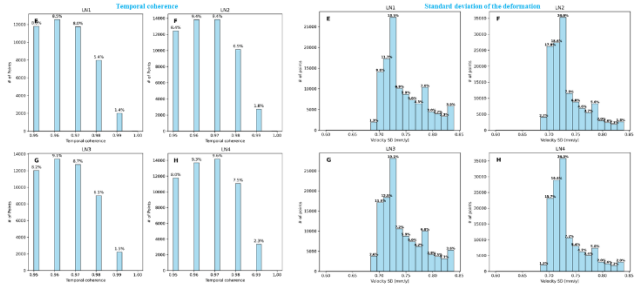

Figure 5. temporal coherence (left) and standard deviation (right) of the PS points of the estimated displacement of TSX data.

3.6.3 Validation

3.6.3.1 Measurements Assessing

Assessing the errors or uncertainty associated with measurements or quantity estimation is determined, take into consideration the steady-state model and assumption of zero subsidence of the stable targets. To give more realistic estimation of the overall error is estimated through determining the error of the velocity(Tarighat et al., 2021) as follow:

$$Error = \sqrt{\left(\frac{std}{\sqrt{k}}\right)^2 + Mean^2} \qquad (3)$$

Whereas the std, mean, and k represent the velocities of standard deviation, the mean value, and the number of the PS points in the

study area, respectively. In this study, conducting and analyzing the results of the experiment helps to assess the error in the measurements and further error analysis of the parameters estimated, to provide precise estimates. As shown in Table 7, the differences in the error values are closer to each other as in the case here, whereas the lowest value appears in LN2 and highest value in LN1 within the time series of two years.

ERROR [mm/yr.]	
Time series	[2014]
Trials	Value
LN1	1.77
LN2	0.41
LN3	0.88
LN4	1.07

Table 7. Error measurement of the estimates of TSX data.

3.6.3.2 GPS comparison

To compare the results of the PSInSAR that measures the displacement in the LOS while the GPS measures the displacement in the three directions East, North, and Up. We need to convert the LOS displacement to the vertical displacement. This can be done with the assumption of the small value of the horizontal movement to be neglected and convert the LOS to vertical displacement using this equation:

$$d_{vertical} = \frac{d_{LOS}}{cos\,\theta}\,, \qquad (4)$$

Where θ = the incidence angle

the four trials and GPS time series for the same time showing the trend values with different values. The trends and patterns of trials are almost like GPS with different trend values. For more accurate validation an interpolation has been applied for the GPS to coincide with the time of PSInSAR time series with a confidence interval covering 68% as shown in Figure 6. with subplot of the four trials and its vertical displacement over time for both PSInSAR and GPS displacement. Each subplot of the four trials display the standard deviation for that trial to GPS Figure 7. The values of standard deviation across all trials identify slight variation of the deviation values, with highest standard deviation value recorded in trial LN4 (3.37 mm) and lowest value in LN3 and LN2 but LN2 is more consistent with the trends and patterns of the GPS.

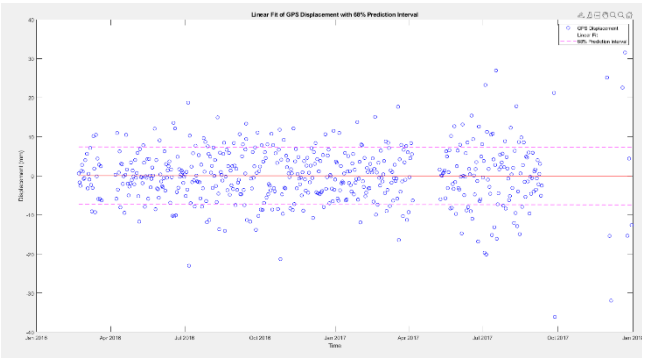

Figure 6. The pink dotted line represent the 68% confidence interval of the GPS vertical displacement.

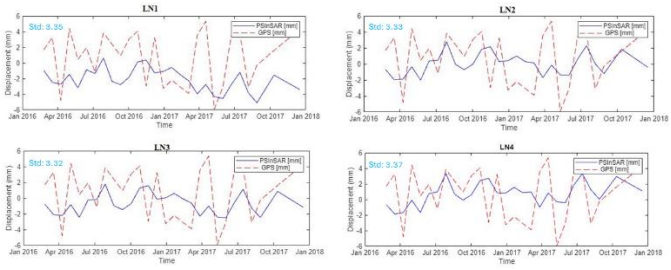

Figure 7. comparison of the selected PS point of PSInSAR data with the interpolated GPS station.

4 Discussion

The standard PSInSAR used in this experiment applied on the same datasets within the same temporal deformation model with the assumption of linear deformation model that employed in this study and indicated from the time series of the PS points as shown in Figure 7. In order to assess the trials with different ranges for both residual height and velocity, The experiment implemented within an area where there is GPS station for assessment of the results. Many factors may affect the deformation results such as noise, model imperfections and unmodelled deformation. As shown in Table 3 the mean of the residuals is negative except for the LN4, indicating the overestimation of the first three trials and underestimation for LN4. In addition, whereas the temporal coherence should be a measure of the fitting to the model and indicator, but it shows not good relation to this and can’t display clear distinction to differentiate between the different parameters range and its response to model fitting. For instance, As shown in Table 4 the median values are the same for the first three trials and become higher at LN4, and when comparing it with another indicator value to check the reliability as shown in Table 6.

The findings suggest that temporal coherence remains unaffected by errors, as evidenced by the higher coefficient of variation (CV) observed in LN2 (CV = 7.88) compared to other trials. Conversely, the CV for standard deviation is lowest at 5.75 at the same trial LN2 compared to other trials, indicating that temporal coherence may not be reliable for assessing errors effects. Additionally, a further investigation, which is uncertainty associated with measurement is determined to assess the quality of the temporal coherence as predictor to fitting. But the results displayed that LN2 has a lower error value compared to other trials as shown in Table 7. These results are consistent with the standard deviation of the deformation rather than temporal coherence. While the temporal coherence is model dependent but insensitive to the errors within the measurements as noticed in the residual values in Table 3.

5 Conclusion

This study investigated the sensitivity of the slight parameter change on the estimation of the deformation velocity and patterns. The experiment is conducted on high resolution SAR images to monitor the slight change in the results accompanied by the different bounds. results of the trials and their assessing throughout the velocity rate and residual height show that even with slight changes in the parameters the PS point velocities show different response, and the estimation could be under- or over-estimated based on the prediction model and the state of deformation model i.e., steady-state model or dynamic model. The results also show that knowledge of deformation behavior is important regarding the avoidance of the nonlinear deformation involvement with wrong implemented model. The most

important results from this experimental study concluded that the temporal coherence that is noise indicator to assessing the fitting to model not good enough to measure the fitting and identifying the errors in the model during selection of PS points.

References

Adam, N., Parizzi, A., Eineder, M., & Crosetto, M., 2009. Practical persistent scatterer processing validation in the course of the Terrafirma project. *Journal of Applied Geophysics*, *69*(1). https://doi.org/10.1016/j.jappgeo.2009.07.002

Afzal, Z., Balz, T., & Asghar, A., 2024. Non-Linear PSInSAR Analysis of Deformation Patterns in Islamabad/Rawalpindi Region: Unveiling Tectonics and Earthquake-Driven Changes. *Remote Sensing*, *16*(7). https://doi.org/10.3390/rs16071194

Bland, J. M., & Altman, D. G., 1996. Statistics Notes: Measurement error. *BMJ*, *313*(7059), 744–744. https://doi.org/10.1136/bmj.313.7059.744

Caro Cuenca, M., J. van Leijen, F., & F. Hanssen, R., 2020. *Shallow subsidence in th Dutch wetlands estimated by satellite radar interferometry*. https://doi.org/10.3997/2214-4609-pdb.150.a01

Ferretti, A., 2014. Satellite InSAR Data: Reservoir Monitoring from Space (EET 9). In *Satellite InSAR Data: Reservoir Monitoring from Space (EET 9)*. https://doi.org/10.3997/9789073834712

Ferretti, A., Prati, C., & Rocca, F., 2000. Nonlinear subsidence rate estimation using permanent scatterers in differential SAR interferometry. *IEEE Transactions on Geoscience and Remote Sensing*, *38*(5 I). https://doi.org/10.1109/36.868878

Ferretti, A., Prati, C., & Rocca, F., 2001. Permanent scatterers in SAR interferometry. *IEEE Transactions on Geoscience and Remote Sensing*, *39*(1), 8–20. https://doi.org/10.1109/36.898661

Hu, J., Motagh, M., Guo, J., Haghighi, M. H., Li, T., Qin, F., & Wu, W., 2022. Inferring subsidence characteristics in Wuhan (China) through multitemporal InSAR and hydrogeological analysis. *Engineering Geology*, *297*. https://doi.org/10.1016/j.enggeo.2022.106530

Jiang, H., Balz, T., Cigna, F., & Tapete, D., 2021. Land Subsidence in Wuhan Revealed Using a Non-Linear PSInSAR Approach with Long Time Series of COSMO-SkyMed SAR Data. *Remote Sensing*, *13*(7). https://doi.org/10.3390/rs13071256

Martone, M., Bräutigam, B., & Krieger, G., 2015. Quantization effects in TanDEM-X data. *IEEE Transactions on Geoscience and Remote Sensing*, *53*(2). https://doi.org/10.1109/TGRS.2014.2325976

Perissin, D., Wang, Z., & Lin, H., 2012. Shanghai subway tunnels and highways monitoring through Cosmo-SkyMed Persistent Scatterers. *ISPRS Journal of Photogrammetry and Remote Sensing*, *73*. https://doi.org/10.1016/j.isprsjprs.2012.07.002

Roccheggiani, M., Piacentini, D., Tirincanti, E., Perissin, D., & Menichetti, M., 2019. Detection and monitoring of tunneling induced ground movements using Sentinel-1 SAR interferometry. *Remote Sensing*, *11*(6). https://doi.org/10.3390/rs11060639

Sousa, J. J., Hooper, A. J., Hanssen, R. F., Bastos, L. C., & Ruiz, A. M., 2011. Persistent Scatterer InSAR: A comparison of methodologies based on a model of temporal deformation vs. spatial correlation selection criteria. *Remote Sensing of Environment*, *115*(10). https://doi.org/10.1016/j.rse.2011.05.021

Tarighat, F., Foroughnia, F., & Perissin, D., 2021. Monitoring of power towers’ movement using persistent scatterer SAR interferometry in south west of Tehran. *Remote Sensing*, *13*(3). https://doi.org/10.3390/rs13030407

Van Leijen, F., 2016. Persistent Scatterer Interferometry based on geodetic estimation theory. In *Climate Change 2013 - The Physical Science Basis* (Vol. 28, Issue 3).

Van Leijen, F. J., & Hanssen, R. F., 2007. Persistent scatterer density improvement using adaptive deformation models. *International Geoscience and Remote Sensing Symposium (IGARSS)*. https://doi.org/10.1109/IGARSS.2007.4423248

Verburg, Q., 2017. *QUInSAR: Temporal Parameter and Ambiguity Estimation Using Recursive Least-Squares*. https://doi.org/10.13140/RG.2.2.36082.27846

Wright, T., Fielding, E., & Parsons, B., 2001. Triggered slip: Observations of the 17 August 1999 Izmit (Turkey) earthquake using radar interferometry. *Geophysical Research Letters*, *28*(6). https://doi.org/10.1029/2000GL011776